Effect of Histidine 6 Protonation on the Active Site Structure and Electron-Transfer Capabilities of Pseudoazurin from *Achromobacter cycloclastes*†

Katsuko Sato and Christopher Dennison*

Department of Chemistry, University of Newcastle upon Tyne, Newcastle upon Tyne, NE1 7RU, U.K.

Received August 31, 2001; Revised Manuscript Received October 31, 2001

ABSTRACT: The paramagnetic ^{1}H NMR spectrum of Cu(II) pseudoazurin [PACu(II)] contains eight directly observed hyperfine-shifted resonances which we have assigned using saturation transfer experiments on a 1:1 mixture of PACu(I) and PACu(II). The spectrum exhibits a number of similarities to those of other cupredoxins, but differences are found concerning the Cu−S(Met) interaction. The spectrum is dependent on pH* in the range 8.5−4.5 (pK_a* 6.4), and a conformational change involving movement of the copper ion away from the Met toward the equatorial ligands, as a consequence of protonation of the surface His6 residue, is identified. Corresponding changes are also seen in the UV/vis spectrum. The protonation/deprotonation equilibrium of His6 influences the reduction potential of the protein in the same pH range. The self-exchange rate constant of PACu at pH* 6.0 (25 °C) is considerably smaller (1.1×10^3 M^{-1} s^{-1}) than the value obtained at pH* 7.6 (3.7×10^3 M^{-1} s^{-1}). The effect on the self-exchange reactivity is mainly due to an alteration in the reorganization energy of the copper site brought about by the structural change resulting from His6 protonation.

Pseudoazurin (PACu)[1] is a type 1 blue copper protein (cupredoxin) which is found in denitrifying bacteria where it can act as the electron donor to a nitrite reductase (NiR) (*1*−*3*). The structures of PACu from *Alcaligenes faecalis* S-6 (*4*−*6*), *Methylobacterium extorquens* AM1 (*7*), *Achromobacter cycloclastes* (*8*), and *Thiosphera pantotropha* (*9*, *10*) have been determined. In all cases the protein contains eight β-strands which form two β-sheets giving an overall β-sandwich topology (see Figure 1). Additionally, pseudoazurin possesses two α-helices which are located at the C-terminus (Figure 1). The single copper ion is buried approximately 5 Å from the protein surface and has a distorted tetrahedral geometry. The copper is strongly coordinated by the N^δ atoms of His40 and His81 and by the thiolate sulfur of Cys78. The copper ion is displaced from the plane of these three equatorial ligands by ∼0.4 Å in the direction of the thioether sulfur of the weak axial Met86 ligand. The His81 ligand of PACu protrudes through a region on the protein's surface made up of nonpolar amino acid residues. Surrounding this hydrophobic patch are a number of basic side chains (see Figure 1). This feature of PACu has been shown to be important for its interaction with NiR (*12*, *13*). Furthermore, since it is known that PACu can interact with a number of different redox partners (*1*−*3*, *14*), this positive hydrophobic surface has been implicated in assisting promiscuous interactions via pseudo-specific docking (*9*).

Type 1 copper centers, such as that found in PACu, have unique spectroscopic features in the cupric state as a consequence of their active site coordination geometry (*15*, *16*). This includes an intense S(Cys) → Cu(II) ligand-to-metal charge transfer (LMCT) transition at approximately 600 nm in their visible spectra, with a second LMCT band at around 450 nm. The EPR spectra of cupredoxins are characterized by having unusually small hyperfine coupling constants in the g_z region, due to the highly covalent nature of the Cu−S(Cys) bond (*15*, *16*). Subtle differences exist in the EPR spectra of type 1 copper sites. Most notably, the difference between the g_x and g_y values can vary, and separations of 0.016 and 0.025 have been found in azurin (*17*) and the green NiR (*18*), respectively. An increase in the difference between the g_x and g_y values gives rise to a more rhombic (less axial) type 1 EPR spectrum. It has been noted that type 1 centers possessing rhombic EPR spectra have increased absorption at around 450 nm in their visible spectra, as compared to those sites with more axial EPR spectra (*15*, *19*−*21*). These observations have led to the classification of type 1 centers as either rhombic or axial with the copper site of PACu belonging to the former group.

Paramagnetic ^{1}H NMR is a technique which has been applied for a number of years to Co(II)- and Ni(II)-substituted cupredoxins and has provided detailed information about their active sites (for example, see refs *22*−*28*). In the past 5 years it has been found that native Cu(II) proteins can also be investigated with this approach (*29*−*35*). The analysis of

† We thank Newcastle University and the Royal Society for funding, CVCP for an ORS award, and EPSRC for a grant to purchase the NMR spectrometer.

* To whom correspondence should be addressed. Tel: +44 191 222 7127. Fax: +44 191 222 6929. E-mail: christopher.dennison@ncl.ac.uk.

[1] Abbreviations: PACu, pseudoazurin; PACu(I), reduced pseudoazurin; PACu(II), oxidized pseudoazurin; LMCT, ligand to metal charge transfer; UV/vis, ultraviolet/visible; NMR, nuclear magnetic resonance; SDS−PAGE, sodium dodecyl sulfate−polyacrylamide gel electrophoresis; 1D, one dimensional; TOCSY, total correlation spectroscopy; WEFT, water-suppressed equilibrium Fourier transform; NHE, normal hydrogen electrode; HEPES, 4-(2-hydroxyethyl)piperazine-1-ethanesulfonic acid; MES, 2-morpholinoethanesulfonic acid; Tris, tris(hydroxymethyl)aminomethane; EPR, electron paramagnetic resonance; pH*, pH meter reading uncorrected for the deuterium isotope effect; HSE, Hahn spin-echo; CPMG, Carr−Purcell−Meiboom−Gill.

10.1021/bi0117448 CCC: $22.00
Published on Web 12/08/2001

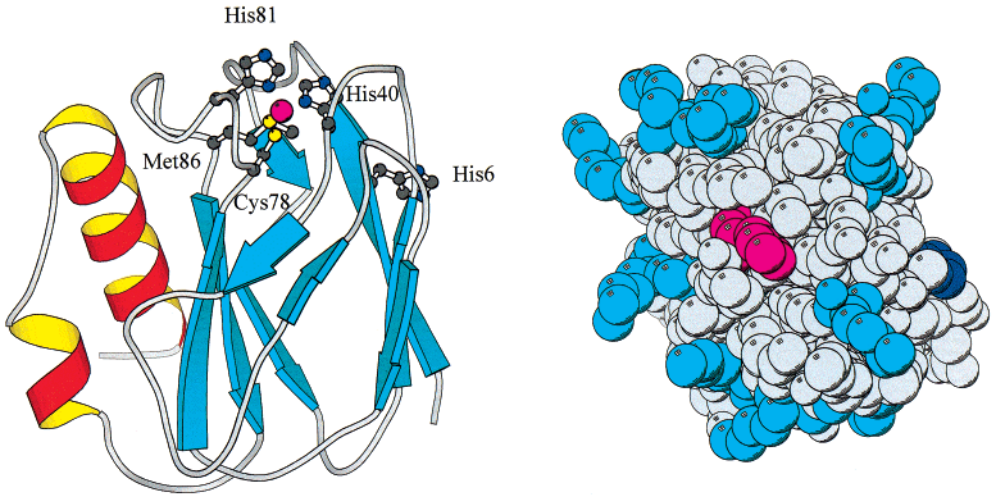

FIGURE 1: Representations of the structure of PACu(II) from *A. cycloclastes* (*8*) (PDB accession code 1BQK) drawn with MOLSCRIPT (*11*). Left: 3D structure with the active site ligands included and the copper ion shown as a magenta sphere. Also indicated is the surface His6 residue. Right: Space-filling model of the hydrophobic surface on PACu through which the ligand His81 (magenta) protrudes. Indicated in light blue are the Lys and Arg residues which surround the hydrophobic patch of PACu, and the surface His6 residue is shown in dark blue.

the copper proteins has the advantage that structural differences caused by the introduction of the non-native metal need not be considered. Additionally, the pseudocontact contribution to the hyperfine shifts is much less for Cu(II), and thus the isotropic shifts provide a good approximation of the Fermi-contact shifts experienced by nuclei (protons) associated with mainly the coordinating residues. The assignment of the peaks is achieved by correlating the broad paramagnetic signals of the Cu(II) protein to their Cu(I) counterparts using exchange spectroscopy on a mixture of the two oxidation states of the protein (*28*, *29*, *31*, *32*, *34*). Due to the relatively long electronic relaxation time of Cu(II) a number of the isotropically shifted resonances at the type 1 site are too broad to be directly observed in the spectra of cupredoxins. An approach using blind saturation transfer experiments, again on mixtures of the Cu(II) and Cu(I) proteins, has allowed such signals, including the $C^{\beta}H$ protons of the Cys ligand, to be indirectly observed (*31*, *32*, *34*). The assigned paramagnetic ^{1}H NMR spectrum of a type 1 Cu(II) center provides detailed information about the coordination geometry and the degree of covalency of the metal ligand bonds (*29*−*35*).

It has long been realized that amino acid residues, whose pK_a values are in the accessible pH range, can have a significant effect on the reactivity of cupredoxins. For example, in certain reduced cupredoxins the exposed His ligand protonates (*6*, *36*, *37*), which has a dramatic effect on the reduction potential (*38*−*41*) and reorganization energy (*42*, *43*) of the protein. In the case of PACu(I) the His81 ligand has been shown to have a pK_a of ∼5.0 (*40*, *44*). Surface, noncoordinated, residues can also have a significant effect on the reactivity of cupredoxins. A well-studied example is *Pseudomonas aeruginosa* azurin, which possesses the exposed His35 residue (*45*). Crystallographic studies (*46*) on the oxidized protein at pH 5.5 and 9.0 have demonstrated a pH-induced conformational change involving a Pro36−Gly37 peptide bond flip. At low pH, the protonated imidazole $N^{\delta 1}$ of His35 forms a strong hydrogen bond with the carbonyl oxygen of Pro36, while at alkaline pH the deprotonated $N^{\delta 1}$ atom acts as an acceptor of a weak hydrogen bond from the amide nitrogen of Gly37. These conformational changes propagate to the active site as His35 is in van der Waals contact with the ligand His46 (*22*, *23*) (it should be noted that significant active site changes are not observed in the crystallographic studies as a consequence of His35 protonation). The protonation/deprotonation equilibrium of His35 influences the reduction potential of *P. aeruginosa* azurin (*47*, *48*). This effect is mainly electrostatic in nature and influences the driving force of electron-transfer reactions with protein redox partners. Pseudoazurin from *A. cycloclastes* possesses a surface-exposed His6 residue (see Figure 1). Crystallographic studies (*8*) on PACu(I) and PACu(II) at pH 6.0 have indicated that Pro35, which is situated close to His6 [6.4 Å between the C^{α} atoms in PACu(II)], undergoes a peptide bond flip in this protein. Although this structural change does not seem to be related to the protonation/deprotonation equilibrium of His6, it results in a reorientation of the imidazole ring of this residue in the two oxidation states of the protein.

In the present study we have investigated the effect of the His6 protonation/deprotonation equilibrium on the structure and reactivity of PACu. This has involved an analysis of the effect of pH on the UV/vis and paramagnetic ^{1}H NMR spectra of PACu(II). To fully understand the effects of pH on the paramagnetic ^{1}H NMR spectrum, we have assigned all of the directly observed signals in the spectrum using saturation transfer experiments on a 1:1 mixture of PACu(II) and PACu(I). The influence of pH on the reduction potential and the self-exchange rate constant have also been investigated. We propose that the protonation/deprotonation equilibrium of the surface His6 residue has a controlling influence on the electron-transfer reactivity of PACu.

EXPERIMENTAL PROCEDURES

Growing A. cycloclastes. A. cycloclastes from a glycerol stock was plated onto fresh LB/agar and incubated at 30 °C until single colonies grew. Cells were transferred into 20 mL of fish extract media (8 g/L Bonito fish extract, 7.5 g/L peptone, 1 g/L yeast extract, 4 g/L KNO_3, 1 g/L NaCl, and

0.01% v/v of a trace metal solution) and incubated at 30 °C for 2−3 days until the culture was fully grown. The 20 mL solution was transferred into 180 mL of fresh media and grown for a further 2−3 days at 30 °C. The fully grown 200 mL culture was transferred to 1.8 L of fresh media and incubated at 30 °C. When this culture was fully grown, the cells were harvested by centrifugation at 13000*g* for 5 min at 4 °C. The pelleted cells were resuspended in 0.8% NaCl solution and centrifuged at 13000*g* for a further 5 min at 4 °C. The supernatant was discarded, and the cells were stored at −20 °C.

Isolation and Purification of PACu. The thawed cells are suspended in 50 mM phosphate buffer, pH 7.0 (1 mL of buffer for 1 g of cells). The solution was sonicated on ice for 30 min. When the cells are completely broken, the solution goes red and turns green upon addition of $K_3[Fe(CN)_6]$ (due to the presence of large amounts of a green copper-containing NiR). After sonication, solutions of $CuSO_4$ and $K_3[Fe(CN)_6]$ were added to the cells (final concentrations approximately 4 and 2 mM, respectively), and the mixture was incubated on ice for 30 min. The solution was spun at 27500*g* for 30 min at 4 °C. Ammonium sulfate was added to the supernatant to a level of 30% saturation (176 g/L), and the resulting solution was left on ice for 30 min and was centrifuged at 27500*g* for 30 min (4 °C). The supernatant was dialyzed against deionized water and then against 20 mM phosphate buffer, pH 6.0. After dialysis particulate matter was removed from the solution by centrifugation at 27500*g* for 30 min (4 °C) and then by passing the supernatant through a 0.2 μm filter. The solution was loaded onto a CM-Sepharose (Pharmacia) column equilibrated with 20 mM phosphate buffer, pH 6.0. The green NiR does not bind to this column, and the column was washed with 20 mM phosphate buffer, pH 6.0, until all of this protein had eluted. Pseudoazurin was eluted with a 0−150 mM NaCl gradient in the same buffer. The PACu-containing fractions were combined, and the NaCl was removed using ultrafiltration (Amicon, 5 kDa MWCO membrane). The protein was loaded onto a CM-Sephadex (Sigma) column equilibrated with 20 mM phosphate buffer, pH 6.0. Pseudoazurin was eluted with a 0−150 mM NaCl gradient in the same buffer. Fractions containing PACu were concentrated to less than 1 mL using ultrafiltration and loaded onto a G-50 gel filtration column (Sigma) equilibrated with 20 mM Tris buffer at pH 7.0 containing 150 mM NaCl. The purity of the protein eluted from this column was checked by UV/vis spectroscopy [pure PACu(II) has a A_{278}/A_{594} ratio of 1.4] and SDS−PAGE.

UV/Vis Spectrophotometry. For UV/vis experiments the protein was fully oxidized using a sufficient volume of a 20 mM solution of $K_3[Fe(CN)_6]$. The excess oxidant was removed using ultrafiltration. The protein was exchanged into 10 mM potassium phosphate buffer. UV/vis spectra were acquired at 25 °C on either a Perkin-Elmer λ 35 or a Shimadzu UV-2101PC spectrophotometer.

Protein Samples for Paramagnetic ^{1}H NMR Studies. For the paramagnetic NMR experiments PACu(II) samples were exchanged into 10 mM potassium phosphate in 99.9% D_2O or 90% H_2O/10% D_2O using centrifugal ultrafiltration units (Centricon 10, Amicon) and typically contained 2−4 mM protein.

PACu(I) Samples for ^{1}H NMR Investigations. PACu was fully reduced by the addition of 1 equivalent of sodium ascorbate, and the protein was exchanged into 10 mM potassium phosphate buffer (99.9% D_2O). The sample was transferred to an NMR tube and flushed with nitrogen. A small amount of sodium ascorbate was added to the sample to maintain the protein in the reduced form.

NMR Sample Preparation for Self-Exchange Rate Constant Measurements. For self-exchange rate constant measurements the sample was exchanged into either 37 mM phosphate at pH* 7.6 or 80 mM phosphate at pH* 6.0 (both with I = 0.10 M). PACu(I) was produced as described above, with the excess reductant exchanged out by ultrafiltration. The reduced sample was placed in an NMR tube, flushed with nitrogen, and sealed. Fully oxidized protein was obtained as described above, and the excess oxidant was removed by ultrafiltration. Small amounts of the oxidized protein were added to the reduced sample. The concentration of the PACu(II) in the sample was determined by transferring the mixed sample to a 2 mm UV/vis cuvette and measuring the absorbance at 594 nm (ϵ = 3700 M^{-1} cm^{-1}) (*49*). Readings were taken before and after the acquisition of NMR spectra, with an average of the two values used for all subsequent calculations (the values usually differed by <0.2% of the total protein concentration).

Protein Samples for the Saturation Transfer Experiments. Saturation transfer experiments were carried out on protein samples in 37 mM phosphate buffer, pH* 7.6. The samples contained equal concentrations (∼ 4 mM) of PACu(I) and PACu(II).

Adjustment of the pH of Protein Samples. The pH values of protein solutions were measured using a narrow pH probe (Russell CMAWL/3.7/180) with an Orion 420A pH meter. The pH of the sample was adjusted using NaOD or DCl in deuterated solutions and NaOH and HCl in H_2O solutions. The pH values quoted in deuterated solutions are uncorrected for the deuterium isotope effect and are indicated by pH*.

NMR Spectroscopy. The ^{1}H NMR spectra were acquired on a JEOL Lambda 500 spectrometer, either using a standard one-pulse sequence employing presaturation of the H_2O or HDO resonance during the relaxation delay or using the super-WEFT pulse sequence (*50*). All chemical shifts are quoted in parts per million (ppm) relative to water using the relationship $\delta_{HDO} = -0.012t + 5.11$ ppm, where t is the temperature in degrees Celsius (*31*). Diamagnetic 1D spectra were acquired with a spectral width of ca. 8 kHz. One-dimensional spectra for the assignment of singlet resonances were acquired using the Hahn spin-echo (HSE) [90°$-\tau-$180°$_y-\tau-$] (τ = 60 ms) and Carr−Purcell−Meiboom−Gill (CPMG) [90°$-\tau-$(180°$_y-2\tau)_n-$180°$_y-\tau$] (n = 59, τ = 1 ms) pulse sequences. Two-dimensional TOCSY spectra of PACu(I) were acquired with mixing times of 70 ms, using a spectral width of ca. 8 kHz with 2048 points for t_2 and 256−512 t_1 increments. Spin−lattice (T_1) relaxation times were determined using a standard inversion recovery sequence ($d-180°-\tau_D-90°-$acq). The values of τ_D ranged from 10 ms to 10 s, with the total relaxation delay (d plus acq) always greater than 5 times the T_1 of the resonances being analyzed. The solvent peak was irradiated during d and τ_D. An exponential fit of a plot of peak intensity against τ_D, for a particular proton, yielded its T_1 value. Spin−spin (T_2) relaxation times were derived from peak widths at half-height using the relation $\nu_{1/2} = (\pi T_2)^{-1}$.

Paramagnetic ^{1}H NMR spectra were acquired with spectral widths ranging from 20 to 100 kHz and were processed with 10−50 Hz exponential line broadening as apodization. Saturation transfer experiments were acquired in the difference mode using a standard one-pulse experiment with irradiation occurring during the relaxation delay. Typically, a relaxation delay of 50 ms was used with an acquisition time of approximately 70−90 ms.

Electrochemistry of PACu. The direct measurement of the reduction potential of PACu was carried out using a Princeton Applied Research model 276 potentiostat operated using software from EG&G. The electrochemical cell consisted of a three-electrode system: a gold working electrode (which was in direct contact with 100−200 μL of a protein-containing solution), a platinum auxiliary electrode, and a Ag/AgCl reference electrode. Measurements were carried out under N_2 and at ambient temperature (21 ± 1 °C) at scan rates of typically 20 mV/s. All reduction potentials were referenced to the NHE, and voltammograms were calibrated using the $[Co(phen)_3]^{3+/2+}$ couple (370 mV vs NHE) (*51*).

Preparation of the Gold Working Electrode. Before each measurement the gold electrode underwent a series of polishing steps crucial to the voltammetric response and was then chemically modified. The electrode was polished using Al_2O_3-coated films, starting with a particle size of 0.3 μm and followed by 0.03 μm film. The electrode was further polished on a slurry of Al_2O_3 (particle size = 0.015 μm) on fresh Buehler cloth. After being polished, the electrode was sonicated in deionized water for at least 1 min. The electrode was rinsed thoroughly with deionized water and then modified by immersion in a saturated solution of 4,4-dithiodipyridine for 2 min. The electrode was thoroughly rinsed after modification with deionized water.

pH and Buffers for Electrochemical Studies. A pH-jump method was used in the range 5.4−8.1 by diluting the protein (10−20-fold) with 20 mM buffer (I = 0.1 M, NaCl). Stock protein solutions (~1−2 mM) were stored in 1 mM HEPES at pH 7.1 (I = 0.1 M, NaCl). For the studies in the pH range 5.4−6.7, MES buffer was used, and Tris was used for the pH range 7.0−8.1.

RESULTS

Effect of pH on the UV/Vis Spectrum of PACu(II). The UV/vis spectrum of PACu(II) is shown in Figure 2A. The main visible absorption band is at 594 nm with a second weaker peak at 452 nm. The ratio of these two bands (A_{452}/A_{594}) is 0.42 at pH 8.0. When the pH value is lowered, the absorption band at 594 nm increases in intensity while that at 452 nm decreases. This results in a A_{452}/A_{594} ratio of 0.36 at pH 5.1 (see Figure 2A). The dependence of the A_{452}/A_{594} ratio on pH is shown in Figure 2B. The data can be fit (three parameters, nonlinear least squares) to eq 1 corresponding to a two-state pH-dependent equilibrium:

$$R = (K_a R_H + [H^+]R_L)/(K_a + [H^+]) \quad (1)$$

where R is the observed A_{452}/A_{594} ratio and R_H and R_L are the corresponding ratios at high and low pH, respectively, yielding a pK_a value of 6.6 ± 0.1 (R_H and R_L values of 0.43 and 0.36, respectively, were obtained from this fit).

Diamagnetic ^{1}H NMR Spectra of PACu(I) and PACu(II). To assign singlet resonances in the diamagnetic ^{1}H NMR spectrum of PACu(I) and PACu(II), a combination of the CPMG and HSE pulse sequences was utilized. In the aromatic region of PACu(I) singlets are identified at 7.79, 7.46, 7.17, 6.97 (two singlets), and 6.80 ppm at 50 °C (pH* 7.6). These singlets must arise from imidazole protons of the two ligand histidines (His40 and His81) and the surface-exposed His6. The peaks at 7.79 and 6.97 exhibit a cross-peak in a TOCSY spectrum as do the resonances at 7.46 and 6.80 ppm and 7.17 and 6.97 ppm, and thus these pairs of singlets can be assigned to particular His residues. The chemical shifts of the signals at 7.79 and 6.97 ppm are dependent on pH* in the range 5−9 and thus can be assigned to the surface His6. The position of the peak at 7.79 ppm is much more sensitive to changes in pH* and is thus assigned to the $C^{\epsilon 1}H$ of His6. The dependence of the chemical shift of this resonance on pH* as measured at 25 °C is shown in Figure 3. A fit of the data to eq 2 yields a pK_a* value of

$$\delta = (K_a \delta_H + [H^+]\delta_L)/(K_a + [H^+]) \quad (2)$$

7.1 ± 0.1. From the dependence on pH* of the ligand His imidazole resonances (*52*) and from the previous observation (*53*) of an NOE between the peaks at 7.46 and 7.17 ppm (which can only arise from the two $C^{\epsilon 1}H$ protons of the His ligands) we can assign the peaks at 7.46 and 6.80 ppm to the His40 $C^{\epsilon 1}H$ and $C^{\delta 2}H$ resonances, respectively, and the signals at 7.17 and 6.97 ppm to the corresponding protons of His81.

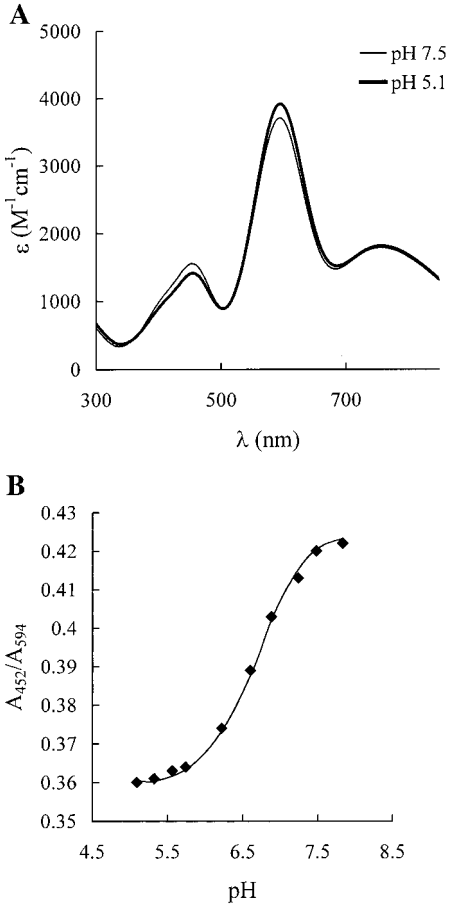

FIGURE 2: (A) Part of the UV/vis spectra (25 °C) of PACu(II) at pH 7.5 and 5.1 in 10 mM phosphate. (B) Dependence on pH (25 °C) of the A_{452}/A_{594} ratio in the visible spectrum of PACu(II) in 10 mM phosphate. The solid lines show the fit of the data to eq 1.

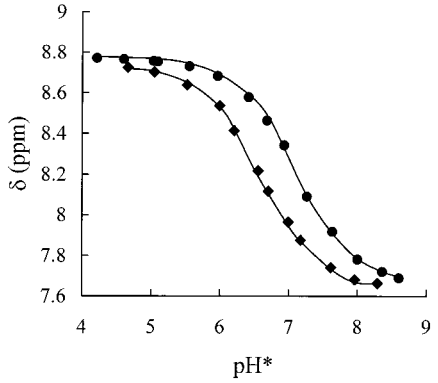

FIGURE 3: Dependence on pH* of the chemical shift of the His6 $C^{\epsilon 1}H$ resonance in the ^1H NMR spectra of PACu(II) (◆) and PACu(I) (●) in 10 mM phosphate (25 °C). The solid lines show fits of the data to eq 2.

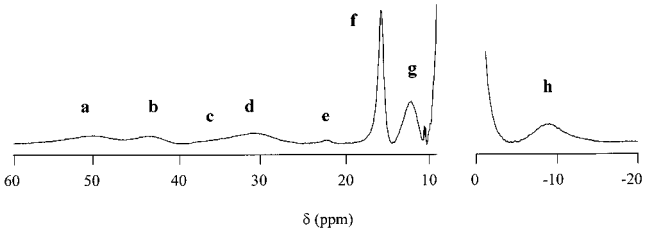

FIGURE 4: ^1H NMR spectrum (50 °C) of PACu(II) (500 MHz) in 10 mM phosphate (99.9% D_2O) at pH* 7.6.

In the aromatic region of the ^1H NMR spectrum of PACu(II) two singlets can be identified at 7.66 and 7.06 ppm at pH* 8.3 (25 °C) and are assigned to His6. The chemical shifts of these peaks are dependent on pH* in the range 8−5 with the peak at 7.66 exhibiting the larger movements with changing pH*. The peak at 7.66 ppm is thus assigned to the $C^{\epsilon 1}H$ of His6, and its dependence on pH* is shown in Figure 3. The data can be fit to eq 2, giving a pK_a* of 6.5 ± 0.1.

Paramagnetic ^1H NMR Spectrum of PACu(II) and Assignment of the Hyperfine-Shifted Resonances. The ^1H NMR spectrum of PACu(II) is shown in Figure 4 and is very similar to that previously reported (*30*). We can directly observe eight hyperfine-shifted resonances (peaks a−h), and we have assigned these using saturation transfer experiments on a 1:1 mixture of PACu(II) and PACu(I). The broad hyperfine-shifted resonances of PACu(II) are irradiated, and saturation transfer is observed to their diamagnetic counterparts in PACu(I). The data obtained when irradiating peaks a, b, f, and g are shown in Figure 5. Listed in Table 1 are results of all of the saturation transfer experiments and the assignments that have been made.

Signals a−d can be assigned to the $C^{\epsilon 1}H$ and $C^{\delta 2}H$ resonances of the two histidine ligands. Peak e, which is an exchangeable resonance but is still observable in the spectrum of the protein in D_2O (Figure 4), has previously been assigned to the $N^{\epsilon 2}H$ proton of the more buried His40 ligand. Spectra were acquired in 90% H_2O/10% D_2O at pH 4.5 and at 5 °C, but the $N^{\epsilon 2}H$ signal of the more exposed His81 ligand is not observed. Irradiation of peak f, which is the least paramagnetic (T_1 ∼5 ms) in the spectrum of PACu(II), leads to saturation transfer to a signal at 4.82 ppm in PACu(I). This indicates that peak f belongs to a $C^{\alpha}H$ resonance. We previously assigned this resonance to the $C^{\alpha}H$ resonance of Cys78, but studies by Bertini et al. (*31*, *32*, *34*) have clearly shown that the peak around 15 ppm in the paramagnetic NMR spectrum of Cu(II) cupredoxins, which has a relatively long T_1 value, arises from the $C^{\alpha}H$ of the Asn residue, which is found adjacent to the N-terminal His ligand. The backbone amide group of this Asn residue hydrogen bonds to the thiolate sulfur of the Cys ligand. We thus assign peak f to the $C^{\alpha}H$ proton of Asn41 in PACu. Irradiation of peak g in PACu(II) leads to the observation of saturation transfer to 0.75 ppm in PACu(I). We previously made a

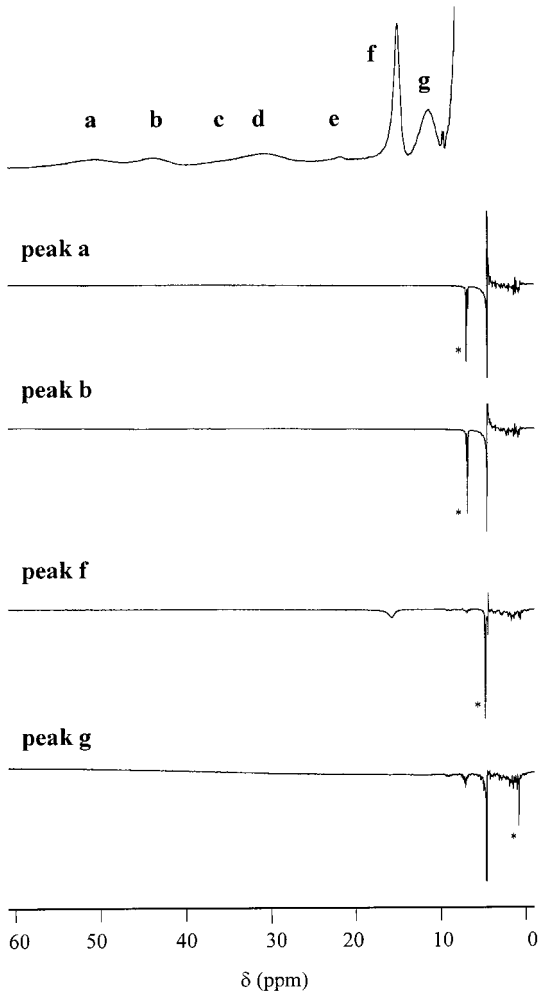

FIGURE 5: ^1H NMR saturation transfer difference spectra (50 °C) of a 1:1 mixture of PACu(I) and PACu(II) in 37 mM phosphate (99.9% D_2O) at pH* 7.6. The top spectrum is that of PACu(II), and those below are the saturation transfer difference spectra in which the peaks indicated were irradiated. The observed saturation transfer peaks in PACu(I) are indicated by an asterisk.

Table 1: Hyperfine-Shifted Resonances of PACu(II) and Their Diamagnetic Counterparts in PACu(I)[a]

resonance	δ_{obs} (ppm) in PACu(II)	δ_{dia} (ppm) in PACu(I)	assignment
a	50.3	6.97	His81 $C^{\delta 2}H$
b	43.7	6.80	His40 $C^{\delta 2}H$
c	∼34	7.17/7.46	His40/81 $C^{\epsilon 1}H$
d	31.1	7.17/7.46	His40/81 $C^{\epsilon 1}H$
e	22.4	nd[b]	His40 $N^{\epsilon 2}H$
f	15.8	4.82	Asn41 $C^{\alpha}H$
g	12.2	0.75	Met86 $C^{\gamma}H$
h	−8.7	5.08	Cys78 $C^{\alpha}H$

[a] Data recorded at 50 °C in 37 mM phosphate buffer (99.9% D_2O) at pH* 7.6. Also included are the assignments that have been made. [b] Not determined.

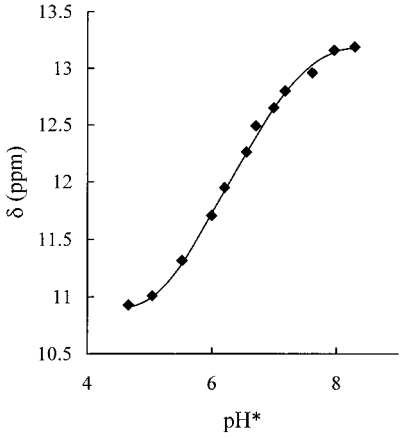

FIGURE 6: Dependence on pH* (25 °C) of the chemical shift of the C$^{\gamma}$H resonance of Met86 in the ^{1}H NMR spectrum of PACu(II) in 37 mM phosphate. The solid line shows a fit of the data to eq 2.

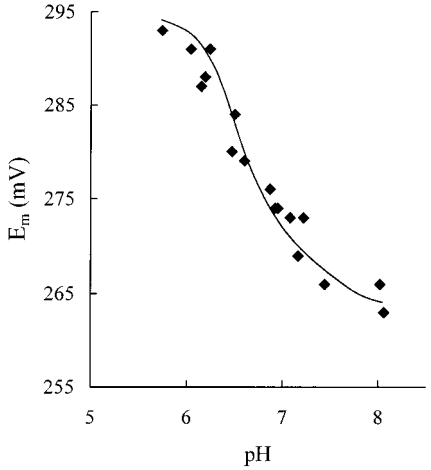

FIGURE 7: Dependence on pH of the reduction potential (E_m) of PACu at $I = 0.10$ M (NaCl). The line shown is obtained from a fit of the data to eq 3.

tentative assignment of peak g as a C$^{\gamma}$H proton of the axial Met86 ligand. The chemical shift observed in PACu(I) is quite unusual for such a proton (typically ~2 ppm). However, in the crystal structure of *A. cycloclastes* PACu (*8*), the side chain of the axial Met86 ligand is positioned very close to the phenyl ring of Phe18, which could result in the upfield shift of the C$^{\gamma}$H proton. Considering the chemical shift value of peak g in PACu(I), an alternative assignment is that it belongs to the C$^{\epsilon}$H$_3$ group of the Met86 ligand. This can be discounted as we have assigned the C$^{\epsilon}$H$_3$ resonance of the Met86 resonance in PACu(I) at 0.64 ppm. Furthermore, the intensity of peak g would clearly argue against it belonging to a methyl group (see Figure 4). Irradiation of peak h in PACu(II) results in saturation transfer to 5.08 ppm in PACu(I). This is consistent with peak g arising from a C$^{\alpha}$H proton, and from a comparison to published data for cupredoxins (*31*, *32*, *34*) we assign this to the Cys78 ligand.

Effect of pH on the Paramagnetic ^{1}H NMR Spectrum of PACu(II).* At pH* 8.3 (25 °C) peak g (Met86 C$^{\gamma}$H) has a chemical shift of 13.2 ppm. When the pH* value is lowered, this peak shifts in an upfield direction, and at pH* 4.7 it is found at 10.9 ppm. The dependence of the chemical shift of peak g on pH* is shown in Figure 6, and the data can be fit to eq 2, yielding a pK_a* value of 6.4 ± 0.2. Peak f exhibits a small dependence on pH* in this range, being found at 17.2 ppm at pH* 8.3 and at 17.3 ppm at pH* 5.0. In spectra obtained on a sample in 90% H_2O/10% D_2O (25 °C) peak e is found at 22.8 ppm at pH 8.1. When the pH is lowered to 4.5, this peak shifts to 23.6 ppm. The remaining peaks in the paramagnetic ^{1}H NMR spectrum of PACu(II) are broader, and thus small changes in their chemical shift are difficult to detect.

pH Dependence of the Reduction Potential of PACu. PACu yielded good, quasi-reversible, responses on a 4,4-dithiodipyridine-modified gold electrode in the pH range 5.7−8.1. In all cases the anodic and cathodic peaks are of equal intensity, and their separation is approximately 60−80 mV at a scan rate of typically 20 mV/s. The peak currents are proportional to the (scan rate)$^{1/2}$ in the range 3−100 mV/s at pH 6.2 ($I = 0.10$ M, NaCl). The reduction potential at pH 8.1 is 263 mV (vs NHE). When the pH value is lowered to 5.7, the reduction potential increases to 293 mV. The dependence of the reduction potential of PACu on pH in this range is shown in Figure 7. The data can be fitted to the equation:

$$E_m(\text{pH}) = E_m(\text{low pH}) + (RT/nF)\ln[(K_a^{red} + [H^+])/(K_a^{ox} + [H^+])] \quad (3)$$

where E_m(pH) is the measured reduction potential, E_m(low pH) is the reduction potential at low pH, K_a^{red} and K_a^{ox} are the proton dissociation constants for the residue in the reduced and oxidized protein, respectively, which influence the E_m(pH) value, and the other symbols have their usual meanings (*54*). The fit of the data to this equation yields pK_a^{red} and pK_a^{ox} values of 6.9 ± 0.2 and 6.3 ± 0.2, respectively.

Effect of pH on the Self-Exchange Rate Constant of PACu As Determined by ^{1}H NMR Spectroscopy.* In a mixture of PACu(I) and PACu(II) the slow exchange condition (*55*−*58*) applies to protons which obey the relationship:

$$k[\text{PACu}]_T \ll 1/T_{i,ox} - 1/T_{i,red} \quad (4)$$

where k is the second-order self-exchange rate constant, $[\text{PACu}]_T$ is the total concentration of protein, and $T_{i,ox}$ and $T_{i,red}$ ($i = 1$ or 2) are the relaxation times for the oxidized and reduced forms, respectively. In these circumstances for dilute solutions containing only a small (<10%) proportion of the oxidized form of the protein it can be shown that the following expression applies (*55*−*58*):

$$1/T_i = (1/T_{i,red}) + k[\text{PACu(II)}] \quad (5)$$

where T_i is the observed relaxation time of the resonance in the reduced protein and [PACu(II)] is the concentration of PACu(II). Thus a plot of T_i^{-1} against [PACu(II)] will give a straight line of slope k.

It is imperative, when determining the self-exchange rate constant of a cupredoxin by ^{1}H NMR spectroscopy, that the protons used be in the slow-exchange regime. In these studies we have used the well-resolved His81 C$^{\epsilon 1}$H and His40 C$^{\epsilon 1}$H resonances. Experiments were carried out at $[\text{PACu}]_T$ values of ~4 mM, and the k values are approximately 1×10^3 to 4×10^3 M^{-1} s^{-1} (vide infra). The $T_{1,red}^{-1}$ values for the resonances used are in the range 0.3−0.5 s^{-1}, while the

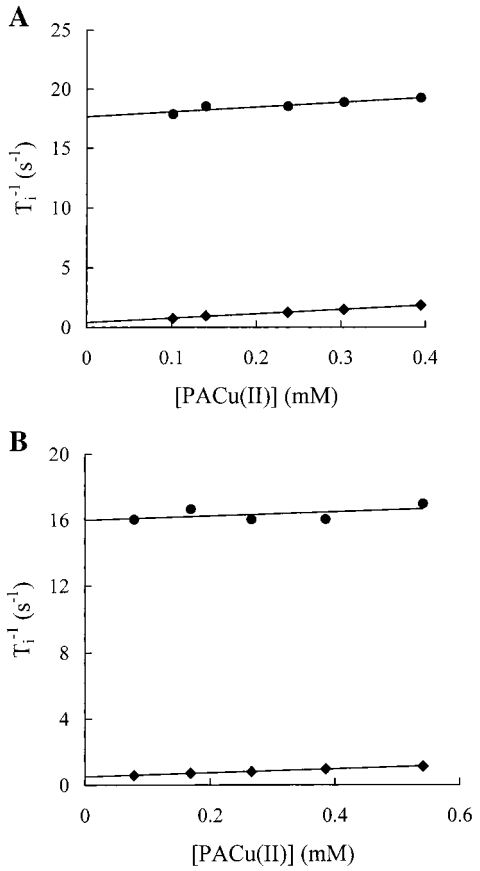

FIGURE 8: Plots of T_1^{-1} (◆) and T_2^{-1} (●) against [PACu(II)] for the $C^{\epsilon 1}H$ signal of His40 (7.59 ppm) at pH* 7.6 (A) and at pH* 6.0 (B).

Table 2: Summary (25 °C) of the Slopes of Plots of T_1^{-1} (k_1) and T_2^{-1} (k_2) against [PACu(II)] in Phosphate Buffer ($I = 0.10$ M)[a]

	His40 $C^{\epsilon 1}H$			His81 $C^{\epsilon 1}H$		
pH*	$k_1/M^{-1}\,s^{-1}$	$k_2/M^{-1}\,s^{-1}$	k_2/k_1	$k_1/M^{-1}\,s^{-1}$	$k_2/M^{-1}\,s^{-1}$	k_2/k_1
7.6	3.6×10^3	4.0×10^3	1.1	3.8×10^3	2.5×10^3	0.7
6.0	1.1×10^3	1.2×10^3	1.1	1.0×10^3	1.3×10^3	1.3

[a] The estimated error in the k_1 values is ±10% while that for the k_2 values is ±20%.

$T_{1,ox}^{-1}$ values of the $C^{\delta 2}H$ and $C^{\epsilon 1}H$ resonances of the His ligands in spinach plastocyanin, an homologous cupredoxin, range from 370 to >1000 s^{-1} (*31*). The $T_{2,red}^{-1}$ values of the PACu peaks used in this study range from 11 to 18 s^{-1}, while the $T_{2,ox}^{-1}$ values are $>7 \times 10^3$ s^{-1} (*31*). Therefore, inequality (*4*) applies to both the T_1 and T_2 data for the peaks used in this study in all of the experiments described. Verification that the protons used belong to the slow-exchange regime is provided by the observation that very similar values of k are found for both the T_1 and T_2 data (vide infra) (*55*, *56*). Furthermore, the observed T_i values are independent of $[PCu]_T$ (*53*), as would be expected to be the case in the slow-exchange regime.

Plots of T_i^{-1} against [PACu(II)] for the $C^{\epsilon 1}H$ signal of His40 at pH* 7.6 (7.59 ppm) and for the same peak at pH* 6.0 (7.59 ppm) are shown in Figure 8. The slopes of these plots (k values) are listed in Table 2 along with the results obtained from the His81 $C^{\epsilon 1}H$ peak (7.25 ppm at pH* 7.6 and 7.27 ppm at pH* 6.0). From the values shown it is clear that the k_2/k_1 ratios (where k_1 and k_2 are the slopes of the plots of T_1^{-1} and T_2^{-1}, respectively, against [PCu(II)]) are all very close to 1, highlighting that these signals are in the slow-exchange regime and thus the k values provide the self-exchange rate constant [k_2/k_1 ratios in excess of 5−10 are expected for protons in the fast-exchange regime (*55*, *56*)]. Due to the small self-exchange rate constant of PACu (in particular at pH* 6.0) the effect of increasing [PCu(II)] on T_2^{-1} is extremely difficult to measure. However, precise measurements of the self-exchange rate constant are readily achieved by measuring the effect of [PACu(II)] on the T_1^{-1} values, and thus the k_1 values provide the more reliable data. Therefore, from an average of the k_1 data of the His40 and His81 $C^{\epsilon 1}H$ signals self-exchange rate constants of 3.7×10^3 and 1.1×10^3 M^{-1} s^{-1} are obtained at pH* 7.6 and 6.0, respectively.

DISCUSSION

Paramagnetic ^1H NMR Spectrum of PACu(II). The 500 MHz paramagnetic ^1H NMR spectrum of PACu(II) reported herein is almost identical to that which was reported earlier at the same field strength (*30*). The use of higher protein concentrations has led to the observation of an additional broad resonance (peak c) at ~34 ppm. Previous tentative assignments relied heavily on a comparison to the assigned spectrum of amicyanin (*29*). We have now carried out saturation transfer experiments on a mixture of oxidized and reduced PACu and assigned all of the directly observed resonances in the spectrum of PACu(II). The observed isotropic shifts (δ_{obs}) for the signals observed for PACu(II) listed in Table 1 arise from three contributing factors as shown in the equation:

$$\delta_{obs} = \delta_{dia} + \delta_{pc} + \delta_{Fc} \quad (6)$$

where δ_{dia} is the observed shift in PACu(I), δ_{pc} is the pseudocontact (through space) contribution, and δ_{Fc} is the Fermi-contact (through-bond) contribution. The pseudocontact shifts are small for protons at a cupric type 1 site (*29*−*32*, *34*, *59*), due to the small anisotropy of the g tensor, and range from ~2 to −2 ppm for the resonances listed in Table 1 (*30*). Therefore, the δ_{obs} values minus the δ_{dia} values for a particular proton listed in Table 1 provide a good estimate of δ_{Fc}, which is a measure of the spin density present on that particular proton.

Peaks a−d are assigned to the two histidine ligands with signals a and b arising from the $C^{\delta 2}H$ protons while peaks c and d are due to the $C^{\epsilon 1}H$ resonances. In all paramagnetic ^1H NMR investigations on Cu(II) cupredoxins to date, these His protons are found in remarkably similar positions (*28*−*35*). This indicates that the spin density distribution onto these two ligands does not vary that much among cupredoxins. The exchangeable $N^{\epsilon 2}H$ signal of the more buried His40 ligand is seen in these studies. Unsuccessful attempts were made at lower pH and temperature to observe the corresponding signal of His81. Therefore, the $N^{\epsilon 2}H$ proton of His81 is in fast exchange with the solvent due to the more solvent-exposed nature of this ligand and is thus broadened beyond detection.

In our previous investigation we incorrectly assigned peak f as the $C^{\alpha}H$ of Cys78 (*30*). The observation herein that both peaks f and h are $C^{\alpha}H$ resonances and studies on other oxidized cupredoxins (*31*, *32*, *34*) have allowed us to assign

peak f as the $C^{\alpha}H$ proton of Asn41, the backbone amide of which hydrogen bonds to the thiolate sulfur of Cys78. Peak h therefore arises from the $C^{\alpha}H$ of the Cys78 ligand. These two peaks are found at very similar positions (∼14−20 ppm for the Asn $C^{\alpha}H$ and ∼−7 to −11 ppm for the Cys $C^{\alpha}H$) in the paramagnetic ^1H NMR spectra of Cu(II) cupredoxins (*29*, *31*−*35*). This indicates that the Fermi-contact shift of these two protons is not that sensitive to the amount of spin density on the thiolate sulfur of the Cys ligand. The position of the $C^{\beta}H$ protons of the Cys ligand provides a sensitive indicator of the spin density on the Cys ligand (*31*, *32*, *34*). In these studies at 500 MHz we have not been able to indirectly observe these protons, unlike in the published studies of plastocyanin (*31*, *34*), azurin, and stellacyanin (*32*) at 800 MHz. However, we have assigned the $C^{\beta}H$ protons of Cys78 in nickel(II) pseudoazurin [data not shown (*52*)]. These are found at 298 and 275 ppm compared to shifts of 296 and 254 ppm and 233 and 187 ppm in nickel(II) amicyanin (*25*) and azurin (*24*), respectively.

Peak g is assigned to the $C^{\gamma}H$ of Met86. The Fermi-contact shift of this resonance (∼10 ppm) provides a measure of the spin density on the thioether sulfur of the axial ligand. In the case of amicyanin Fermi-contact shifts of 7.3 and 6.7 ppm are observed (*29*) whereas in spinach plastocyanin (*31*) values of 19.9 and 8.6 ppm are found (in both proteins the value for the $C^{\gamma 2}H$ proton is quoted first). In the plastocyanin from the cyanobacterium *Synechocystis* PCC 6803 only the $C^{\gamma 2}H$ proton is observed with a Fermi-contact shift of 20.0 ppm (*34*) while in azurin neither of the $C^{\gamma}H$ protons of the axial Met are shifted outside of the diamagnetic envelope (*29*, *52*). We assume that the second $C^{\gamma}H$ of Met86 in PACu(II) is not shifted outside of the diamagnetic region of the spectrum.

The above comparisons of the isotropic shifts experienced by the Cys $C^{\beta}H$ protons and Met $C^{\gamma}H$ signals in paramagnetic cupredoxins indicate that the active site architecture of PACu is very similar to that of amicyanin. However, PACu has a type 1 rhombic site whereas that of amicyanin (and plastocyanin) is type 1 axial. It has been proposed (*19*, *20*) that this distinction is based on movement of the copper ion relative to the plane of the three equatorial ligands, thus altering the strength of the axial Cu−S(Met) bond, with an enhanced axial interaction resulting in a more rhombic type 1 site. A stronger axial interaction is also thought to result in a lengthening of the equatorial Cu−S(Cys) bond (*21*). The Cu−S(Met) bond length is similar in PACu (2.71 Å) (*8*), plastocyanin (2.88 Å) (*60*), and amicyanin (2.84 Å) (*61*) but is significantly longer in azurin (3.15 Å) (*46*). It therefore appears that active site differences which do not influence the paramagnetic ^1H NMR spectra of the cupredoxins and which cannot be attributed to variations in Cu−S(Met) bond lengths, can also influence the fine details of the EPR and UV/vis spectra. It may be that, as suggested in recent theoretical studies (*62*−*64*), angular changes in the positions of the ligands affect the spectral features of a type 1 copper site. Such differences may also be responsible for the quite dramatic variation in spectroscopic properties between the type 1 sites of blue and green copper-containing NiRs despite them having similar Cu−S(Cys) and Cu−S(Met) bond lengths (*33*). It should be remembered when making comparisons that the Fermi-contact shifts observed in the paramagnetic NMR spectra exhibit angular dependencies. For example, Bertini et al. have proposed (*31*) that the Fermi-contact shifts of the Cys $C^{\beta}H$ protons can be interpreted considering a $\sin^2\theta$ dependence on the Cu−S−C^{β}−H^{β} dihedral angle. [It should be noted that in nickel(II) and cobalt(II) azurin a $\cos^2\theta$ dependence on the M−S−C^{β}−H^{β} dihedral angle has been reported (*26*) for the Fermi-contact shifts of the Cys $C^{\beta}H$ protons.] Studies are currently underway to further investigate this aspect of the paramagnetic NMR spectra of cupredoxins.

The pK_a values of His6 in PACu(I) and PACu(II) Determined by ^1H NMR Spectroscopy*. The pK_a* values that we obtain in this investigation for His6 [7.1 ± 0.1 and 6.5 ± 0.1 for PACu(I) and PACu(II), respectively] are in good agreement with those determined previously (*40*). The pK_a value of His6 is influenced by the oxidation state of the copper in PACu. As expected, the presence of an additional positive charge on the metal ion results in a decrease in the pK_a for the surface His. The magnitude of the difference in the pK_a of His6 in PACu(I) and PACu(II) is consistent with the distance between this residue and the copper (14.8 Å between the copper and the N^{ϵ} of His6) and the effect being mainly electrostatic in nature (*47*, *65*). However, the structural changes that are seen in the crystallographic studies of PACu around His6 upon reduction (*8*) may also influence the pK_a value of this residue. The effect of the oxidation state of the copper on the pK_a of His6 results in an approximately 30 mV effect on the reduction potential over the pH range 8 to ∼5.5 (vide infra).

Effect of pH on the UV/Vis Spectrum of PACu(II). The changes in the visible spectrum of PACu(II) in the pH range 5−8 (pK_a 6.6 ± 0.1) indicate that the protonation/deprotonation equilibrium of the surface His6 results in a structural change at the active site. The visible spectrum at low pH is indicative of a less rhombic type 1 center under these conditions (decrease in the A_{452}/A_{594} ratio). EPR and resonance Raman spectra of PACu(II) at pH 8 and 5 do not exhibit any discernible differences (data not shown). The EPR spectra were obtained at 77 K, which could alter the equilibrium between the protonated and deprotonated forms of PACu(II). Furthermore, previous studies have shown that resonance Raman spectroscopy is relatively insensitive to subtle structural differences at type 1 centers (*47*, *66*−*68*). However, the results of paramagnetic ^1H NMR studies also indicate a more axial type 1 site in PACu(II) at acidic pH values (vide infra). The changes observed in the visible spectrum in these studies are very similar to those previously observed above pH 9 for PACu(II) (*30*, *49*). This alkaline transition (pK_a ∼10.3) has been assigned to a surface lysine residue situated close to the copper site and results in the A_{452}/A_{594} ratio decreasing to 0.35 at pH 11.

This is the first reported case in a cupredoxin where the protonation/deprotonation equilibrium of a surface histidine residue has an effect on the visible spectrum of the protein. Therefore, we have also studied the effect of pH on the visible spectra of azurin from *P. aeruginosa*, which has surface histidines at positions 35 and 83 (*45*), and the plastocyanins from the green algae *Scenedesmus obliquus* and the cyanobacterium *Synechococcus* sp. PCC 7942, which have uncoordinated surface His57 residues (*69*, *70*). In all cases the visible spectrum is unaltered in the pH range 9−4 (the pK_a values for the surface His residues are all in this pH region). This is particularly noteworthy in the case of

azurin as His35 protonation/deprotonation is known to affect the structure and reactivity of the protein (vide supra; *46*−*48*, *71*). In particular, it has been demonstrated that protonation of this residue affects the active site structure of azurin (*22*, *23*). However, this modification of the active site does not alter the visible spectrum of the protein. This would tend to indicate that the active site changes induced by the protonation of His6 in PACu are larger than those caused by the ionization of His35 in azurin. Alternatively, it could be that the pH-induced active site fluxionality in PACu(II) has more of an influence on the Cu−S(Cys) bond, which is of key importance for the visible spectral features of a type 1 copper site (*15*, *16*).

Effect of pH on the Paramagnetic ^{1}H NMR Spectrum of PACu(II).* When the pH* is lowered from ∼8, changes are observed in the paramagnetic ^{1}H NMR spectrum of PACu(II). The C$^\gamma$H resonance of Met86 shifts in an upfield direction, and the pK_a* value obtained (6.4 ± 0.2) indicates that this effect is due to the protonation of His6. Additionally, the His40 N$^{\epsilon 2}$H signal shifts in a downfield direction when the pH value is lowered. Thus the protonation of His6 leads to a change in the structure of the copper site which results in an approximately 20% decrease in the Fermi-contact shift of the Met86 C$^\gamma$H proton. This is consistent with an increase in the Cu−S(Met) bond length and consequently a decrease in the amount of spin density on the thioether sulfur of this residue. The increased δ_{obs} value of the His40 N$^{\epsilon 2}$H proton corresponds to an ∼5−10% increase in the Fermi-contact shift of this resonance. It therefore appears that the protonation of His6 results in the movement of the copper ion away from the axial Met86 toward the plane of the three equatorial ligands. This explanation is in agreement with the effect seen in the visible spectrum of PACu(II), where a more axial type 1 site appears to prevail at acidic pH values. These changes in the paramagnetic ^{1}H NMR spectrum of PACu(II) are very similar to those resulting from the alkaline transition (*30*). Thus both of the observed pH-induced active site transitions in PACu(II) result in a similar effect on the active site structure.

Effect of pH on the Reduction Potential of PACu. The effect of pH on the reduction potential in the range 8.1−5.7 yields pK_a^{ox} and pK_a^{red} values which correspond to those determined for His6 in PACu(II) and PACu(I), respectively, in the NMR studies. The protonation/deprotonation equilibrium of His6 has an effect on the reduction potential of PACu, and this appears to be mainly electrostatic in nature. This increase in the reduction potential will result in PACu(I) being a less efficient reductant of its physiological electron-transfer partner (NiR). At even more acidic pH values it is known that the ligand His81 protonates in PACu(I) (*6*, *40*, *44*), which has a much more dramatic effect on the protein's reduction potential and its electron-transfer reactivity.

Effect of pH on the Self-Exchange Rate Constant of PACu. The self-exchange rate constant of PACu determined at pH* 7.6 (3.7×10^3 M^{-1} s^{-1}) is almost the same as that determined previously under identical conditions [3.5×10^3 M^{-1} s^{-1} at pH* 8.2 (*30*) and 2.9×10^3 M^{-1} s^{-1} at pH* 7.5 (*53*)]. However, the present measurement, which has involved the analysis of T_1 data, provides a much more precise value. An alternative approach for the determination of self-exchange rate constants of cupredoxins has been published (*72*, *73*). This utilizes super-WEFT spectra of partially oxidized samples to determine the broadening of fast relaxing peaks arising from the reduced protein. However, this method is only suitable if the self-exchange rate constant is large. The self-exchange rate constant for PACu is quite small and is at the low end of the range observed for cupredoxins (*42*, *55*, *56*, *74*, *75*), and thus this method cannot be applied. The hydrophobic patch surrounding the exposed His ligand is a conserved feature of all structurally characterized cupredoxins (*76*, *77*). It has been demonstrated that the hydrophobic patch is used for association prior to self-exchange in cupredoxins (*30*, *47*, *48*, *78*) and also in reactions with physiological electron-transfer partners (*79*−*81*). Furthermore, the exposed His ligand is thought to be the conduit for electron transfer (*82*−*84*). In the case of PACu the positively charged residues which surround the hydrophobic patch (see Figure 1) hinder protein−protein association and thus result in the small self-exchange rate constant for this cupredoxin. The self-exchange rate constant determined at pH* 6.0, at which value His6 will be mainly protonated in both PACu(I) and PACu(II) and at which the protonation of the His81 ligand in PACu(I) will not be influential, is ∼3.5 times less (1.1×10^3 M^{-1} s^{-1}) than that at pH* 7.6. The effect of His6 protonation on the self-exchange rate constant equates to an approximately 100 meV increase in the reorganization energy of the copper site, an ∼3 kJ/mol decrease in the Gibbs free energy of association of two PACu molecules or a ca. 1 Å increase in the distance for electron transfer. In Figure 1 it can be seen that His6 is quite far from the copper site and the exposed His81 ligand. This, and the large number of lysine residues around the hydrophobic patch of PACu, would tend to indicate that the presence of an extra positive charge at His6 would not greatly affect the association of two PACu molecules. It is also unlikely that protonation of His6 would significantly alter the distance for electron transfer in the self-exchange reaction of PACu. We therefore conclude that the smaller self-exchange rate constant at lower pH* can be attributed to a larger reorganization energy as a consequence of the active site alterations caused by the protonation of His6. Considering that the reorganization energies of type 1 centers are ∼1 eV (*85*, *86*), the calculated increase (∼100 meV) is approximately the magnitude of alteration one would expect considering the spectroscopic changes induced by this transition. This explanation is consistent with the results of kinetic studies of the oxidation of PACu(I) by the inorganic complexes $[Co(phen)_3]^{3+}$ and $[Co(dipic)_2]^-$ (*40*). The second-order rate constants for these reactions exhibit quite marked dependence on pH in the range 8−6 (decreasing on going to lower pH). These effects would appear to be too large to be attributed to a decrease in the driving force alone for the reactions (due to the increase in the E_m value of PACu in this pH range) and must be partly due to the increase in the reorganization energy at low pH as a result of the protonation of His6.

The alkaline transition of PACu also has a dramatic effect on the self-exchange rate constant of PACu (*30*). The value obtained at pH* 11.3 is ∼10 times greater than that at pH* 7.6. In this case the deprotonation of the surface Lys residues at the more alkaline pH* values facilitates protein−protein association. This far outweighs any effect the alkaline transition has on the reorganization energy of the copper center. The pK_a value for this transition (∼10.3) indicates that this effect is of no physiological relevance. The influence

that His6 exhibits on the reactivity of PACu occurs at a pH value at which PACu will function in vivo. We can therefore assume that the observed effect may be utilized to control the reactivity of PACu with its physiological electron-transfer partners. Studies on *P. aeruginosa* azurin have shown that its self-exchange rate constant is almost independent of pH (*47*, *55*). Thus the protonation of His35, which is much closer to the copper site (8.3 Å from the copper to the $N^{\delta 1}$ atom), has only a minor effect in this protein. The buried nature of His35 prevents the protonation of this residue, having an electrostatic influence on the association of two azurin molecules. This is therefore consistent with the more limited effects that protonation of His35 has on the spectroscopic properties of the protein and with the suggestions that it results in a more limited alteration of the active site structure.

CONCLUSIONS

The assignment of the paramagnetic ^{1}H NMR spectrum of PACu provides detailed information about the active site of this cupredoxin. The active site architecture of PACu seems to be very similar to that of amicyanin regardless of differences in the EPR and UV/vis spectra of these two proteins (amicyanin has a type 1 axial site whereas PACu's is type 1 rhombic). The effect of the protonation/deprotonation equilibrium of His6 on the paramagnetic NMR spectrum identifies the nature of the resulting structural changes at the active site. At low pH the metal ion at the active site of PACu(II) has moved away from the axial Met86 toward the three equatorial ligands. The observed effects on the UV/vis spectrum in the same pH range (decreased A_{452}/A_{594} ratio upon lowering pH) indicate that one reason for the enhanced absorption around 450 nm in the spectra of cupredoxins is an increased Cu−S(Met) interaction.

The protonation/deprotonation of His6 has a Coulombic effect on the copper site resulting in a modification of the reduction potential. This provides one mechanism whereby pH can tune the reactivity of this cupredoxin. The protonation of His6 results in an ∼3.5-fold decrease in the self-exchange rate constant of PACu. We suggest that this is mainly due to an increase in the reorganization energy of the copper site at low pH. This conclusion highlights another mechanism for controlling the electron-transfer reactivity of this cupredoxin. These effects are quite subtle compared to the effect His81 protonation has on the reduction potential and reorganization energy of the protein. The latter effect consequently prevents electron transfer of PACu with its physiological partners whereas the protonation/deprotonation equilibrium of His6 fine-tunes the reactivity.

ACKNOWLEDGMENT

We thank Prof. T. Kohzuma (Ibaraki University, Japan) for providing the bacterial strain and for assistance with EPR and UVRR experiments and Prof. T. Kitagawa (Institute for Molecular Science, Okazaki, Japan) for access to resonance Raman facilities.

REFERENCES

1. Kakutami, T., Watanabe, H., Arima, K., and Beppu, T. (1981) *J. Biochem. 89*, 463−472.
2. Liu, M. Y., Liu, M. C., Payne, W. J., and Legall, J. (1986) *J. Bacteriol. 166*, 604−608.
3. Moir, J. W. B., Baratta, D., Richardson, D. J., and Ferguson, S. J. (1993) *Eur. J. Biochem. 212*, 377−385.
4. Petratos, K., Dauter, Z., and Wilson, K. S. (1988) *Acta Crystallogr. B44*, 628−636.
5. Adman, E. T., Turley, S., Bramson, R., Petratos, K., Banner, D., Tsernoglou, D., Beppu, T., and Watanabe, H. (1989) *J. Biol. Chem. 264*, 87−99.
6. Vakoufari, E., Wilson, K. S., and Petratos, K. (1994) *FEBS Lett. 347*, 203−206.
7. Inoue, T., Kai, Y., Harada, S., Kasai, N., Ohshiro, Y., Suzuki, S., Kohzuma, T., and Tobari, J. (1994) *Acta Crystallogr. D50*, 317−328.
8. Inoue, T., Nishio, N., Suzuki, S., Kataoka, K., Kohzuma, T., and Kai, Y. (1999) *J. Biol. Chem. 274*, 17845−17852.
9. Williams, P. A., Fülöp, V., Leung, Y. C., Chan, C., Moir, J. W. B., Howlett, G., Ferguson, S. J., Radford, S. E., and Hajdu, J. (1999) *Nat. Struct. Biol. 2*, 975−982.
10. Thompson, G. S., Leung, Y. C., Ferguson, S. J., Radford, S. E., and Redfield, C. (2000) *Protein Sci. 9*, 846−858.
11. Kraulis, P. J. (1991) *J. Appl. Crystallogr. 24*, 946−950.
12. Kukimoto, M., Nishiyama, M., Tanokura, M., Adman, E. T., and Horinouchi, S. (1996) *J. Biol. Chem. 271*, 13680−13683.
13. Kukimoto, M., Nishiyama, M., Ohnuki, T., Turley, S., Adman, E. T., Horinouchi, S., and Beppu, T. (1995) *Protein Eng. 8*, 153−158.
14. Moir, J. W. B., and Ferguson, S. J. (1994) *Microbiology 140*, 389−397.
15. Canters, G. W., and Gilardi, G. (1993) *FEBS Lett. 325*, 39−48.
16. Solomon, E. I., Penfield, K. W., Gewirth, A. A., Lowery, M. D., Shadle, S. E., Guckert, J. A., and LaCroix, L. B. (1996) *Inorg. Chim. Acta 243*, 67−78.
17. Coremans, J. W. A., Poluektov, O. G., Groenen, E. J. J., Canters, G. W., Nar, H., and Messerschmidt, A. (1994) *J. Am. Chem. Soc. 116*, 3097−3101.
18. van Gastel, M., Boulanger, M. J., Canters, G. W., Huber, M., Murphy, M. E. P., Verbeet, M. Ph., and Groenen, E. J. J. (2001) *J. Phys. Chem. B 105*, 2236−2243.
19. Han, J., Loehr, T. M., Lu, Y., Valentine, J. S., Averill, B. A., and Sanders-Loehr, J. (1993) *J. Am. Chem. Soc. 115*, 4256−4263.
20. Lu, Y., LaCroix, L. B., Lowery, M. D., Solomon, E. I., Bender, C. J., Peisach, J., Roe, J. A., Gralla, E. B., and Valentine, J. S. (1993) *J. Am. Chem. Soc. 115*, 5907−5918.
21. Andrew, C. R., Yeom, H., Valentine, J. S., Karlsson, B. G., Bonander, N., van Pouderoyen, G., Canters, G. W., Loehr, T. M., and Sanders-Loehr, J. (1994) *J. Am. Chem. Soc. 116*, 11489−11498.
22. Moratal, J. M., Salgado, J., Donaire, A., Jiménez, H. R., and Castells, J. (1993) *Inorg. Chem. 32*, 3587−3588.
23. Moratal, J. M., Salgado, J., Donaire, A., Jiménez, H. R., and Castells, J. (1993) *J. Chem. Soc., Chem. Commun.*, 110−112.
24. Salgado, J., Jiménez, H. R., Moratal, J. M., Kroes, S., Warmerdam, G. C. M., and Canters, G. W. (1996) *Biochemistry 35*, 1810−1819.
25. Salgado, J., Kalverda, A. P., Diederix, R. E. M., Canters, G. W., Moratal, J. M., Lawler, A. T., and Dennison, C. (1999) *J. Biol. Inorg. Chem. 4*, 457−467.
26. Donaire, A., Salgado, J., and Moratal, J. M. (1998) *Biochemistry 37*, 8659−8673.
27. Vila, A. J., and Fernández, C. O. (1996) *J. Am. Chem. Soc. 118*, 7291−7298.
28. Salgado, J., Kroes, S. L., Berg, A., Moratal, J. M., and Canters, G. W. (1998) *J. Biol. Chem. 273*, 177−185.
29. Kalverda, A. P., Salgado, J., Dennison, C., and Canters, G. W. (1996) *Biochemistry 35*, 3085−3092.
30. Dennison, C., and Kohzuma, T. (1999) *Inorg. Chem. 38*, 1491−1497.
31. Bertini, I., Ciurli, S., Dikiy, A., Gasanov, R., Luchinat, C., Martini, G., and Safarov, N. (1999) *J. Am. Chem. Soc. 121*, 2037−2046.
32. Bertini, I., Fernández, C. O., Karlsson, B. G., Leckner, J., Luchinat, C., Malmström, B. G., Nersissian, A. M., Pierattelli, R., Shipp, E., Valentine, J. S., and Vila, A. J. (2000) *J. Am. Chem. Soc. 122*, 3701−3707.

33. Dennison, C., Oda, K., and Kohzuma, T. (2000) *Chem. Commun*., 751−752.
34. Bertini, I., Ciurli, S., Dikiy, A., Fernandez, C. O., Luchinat, C., Safarov, N., Shumilin, S., and Vila, A. J. (2001) *J. Am. Chem. Soc. 123*, 2405−2413.
35. Dennison, C., and Lawler, A. T. (2001) *Biochemistry 40*, 3158−3166.
36. Guss, J. M., Harrowell, P. R., Murata, M., Norris, V. A., and Freeman, H. C. (1986) *J. Mol. Biol. 192*, 361−387.
37. Zhu, Z., Cunane, L. M., Chen, Z. W., Durley, R. C. E., Mathews, F. S., and Davidson, V. L. (1998) *Biochemistry 37*, 17128−17136.
38. Katoh, S., Shiratori, I., and Takamiya, A. (1962) *J. Biochem. 51*, 32−40.
39. Armstrong, F. A., Hill, H. A. O., Oliver, B. N., and Whitford, D. (1985) *J. Am. Chem. Soc. 107*, 1473−1476.
40. Dennison, C., Kohzuma, T., McFarlane, W., Suzuki, S., and Sykes, A. G. (1994) *Inorg. Chem. 33*, 3299−3305.
41. Dennison, C., Vijgenboom, E., Hagen, W. R., and Canters, G. W. (1996) *J. Am. Chem. Soc. 118*, 7406−7407.
42. Lommen, A., and Canters, G. W. (1990) *J. Biol Chem. 265*, 2768−2774.
43. Di Bilio, A. J., Dennison, C., Gray, H. B., Ramirez, B. E., Sykes, A. G., and Winkler, J. R. (1998) *J. Am. Chem. Soc. 120*, 7551−7556.
44. Dennison, C., Kohzuma, T., McFarlane, W., Suzuki, S., and Sykes, A. G. (1994) *J. Chem. Soc., Chem. Commun*., 581−582.
45. Kolczak, U., Dennison, C., Messerschmidt, A., and Canters, G. W. (2001) in *Handbook of Metalloproteins* (Messerschmidt, A., Huber, R., Poulos, T., and Wieghardt, K., Eds.) pp 1170−1194, John Wiley & Sons, Chichester.
46. Nar, H., Messerschmidt, A., Huber, R., van de Kamp, M., and Canters, G. W. (1991) *J. Mol. Biol. 221*, 765−772.
47. van de Kamp, M., Canters, G. W., Andrew, C. R., Sanders-Loehr, J., Bender, C. J., and Peisach, J. (1993) *Eur. J. Biochem. 218*, 229−238.
48. van Pouderoyen, G., Mazumdar, S., Hunt, N. I., Hill, H. A. O., and Canters, G. W. (1994) *Eur. J. Biochem. 222*, 583−588.
49. Kohzuma, T., Dennison, C., McFarlane, W., Nakashima, S., Kitagawa, T., Inoue, T., Kai, Y., Nishio, N., Shidara, S., Suzuki, S., and Sykes, A. G. (1995) *J. Biol. Chem. 270*, 25733−25738.
50. Inubushi, T., and Becker, E. D. (1983) *J. Magn. Reson. 51*, 128−133.
51. Paglia, B., and Sirani, C. (1957) *Gazz. Chim. Ital. 81*, 1125−1132.
52. Sato, K., and Dennison, C., unpublished results.
53. Dennison, C., Kohzuma, T., McFarlane, W., Suzuki, S., and Sykes, A. G. (1994) *J. Chem. Soc., Dalton Trans.*, 437−443.
54. Clark, W. M. (1960) *Oxidation−Reduction Potentials of Organic Systems*, Waverley Press, Baltimore, MD.
55. Groeneveld, C. M., and Canters, G. W. (1988) *J. Biol. Chem. 263*, 167−173.
56. Dennison, C., Kyritsis, P., McFarlane, W., and Sykes, A. G. (1993) *J. Chem. Soc., Dalton Trans.*, 1959−1963.
57. Leigh, J. S. (1971) *J. Magn. Reson. 4*, 308−311.
58. McLaughlin, A. C., and Leigh, J. S. (1973) *J. Magn. Reson. 9*, 296−304.
59. Ubbink, M., Lian, L. Y., Modi, S., Evans, P. A., and Bendall, D. S. (1996) *Eur. J. Biochem. 242*, 132−147.
60. Xue, Y., Ökvist, M., Hansson, O., and Young, S. (1998) *Protein Sci. 7*, 2099−2105.
61. Romero, A., Nar, H., Huber, R., Messerschmidt, A., Kalverda, A. P., Canters, G. W., Durley, R., and Mathews, F. S. (1994) *J. Mol. Biol. 236*, 1196−1211.
62. LaCroix, L. B., Shadle, S. E., Wang, Y., Averill, B. A., Hedman, B., Hodgson, K. O., and Solomon, E. I. (1996) *J. Am. Chem. Soc. 118*, 7755−7768.
63. Pierloot, K., De Kerpel, J. O. A., Ryde, U., Olsson, M. H. M., and Roos, B. O. (1998) *J. Am. Chem. Soc. 120*, 13156−13166.
64. LaCroix, L. B., Randall, D. W., Nersissian, A. M., Hoitink, C. W. G., Canters, G. W., Valentine, J. S., and Solomon, E. I. (1998) *J. Am. Chem. Soc. 120*, 9621−9631.
65. Bashford, D., Karplus, M., and Canters, G. W. (1988) *J. Mol. Biol. 203*, 507−510.
66. den Blaauwen, T., Hoitink, C. W. G., Canters, G. W., Han, J., Loehr, T. M., and Sanders-Loehr, J. (1993) *Biochemistry 32*, 12455−12464.
67. Buning, C., Canters, G. W., Comba, P., Dennison, C., Jeuken, L., Melter, M., and Sanders-Loehr, J. (2000) *J. Am. Chem. Soc. 122*, 204−211.
68. Nersissian, A. M., Mehrabian, Z. B., Nalbandyan, R. M., Hart, P. J., Fraczkiewicz, G., Czernuszewicz, R. S., Bender, C. J., Peisach, J., Herrmann, R. G., and Valentine, J. S. (1996) *Protein Sci. 5*, 2184−2192.
69. Moore, J. M., Chazin, W. J., Powls, R., and Wright, P. E. (1988) *Biochemistry 27*, 7806−7816.
70. Inoue, T., Sugawara, H., Hamanaka, S., Tsukui, H., Suzuki, E., Kohzuma, T., and Kai, Y. (1999) *Biochemistry 38*, 6063−6069.
71. Kalverda, A. P., Ubbink, M., Gilardi, G., Wijmenga, S. S., Crawford, A., Jeuken, L. J. C., and Canters, G. W. (1999) *Biochemistry 38*, 12690−12697.
72. Ma, L., Philipp, E., and Led, J. J. (2001) *J. Biomol. NMR 19*, 199−208.
73. Salgado, J., Kalverda, A. P., and Canters, G. W. (1997) *J. Biomol. NMR 9*, 299−305.
74. Kyritsis, P., Dennison, C., Ingledew, W. J., McFarlane, W., and Sykes, A. G. (1995) *Inorg. Chem. 34*, 5370−5374.
75. Hunter, D. M., McFarlane, W., Sykes, A. G., and Dennison, C. (2001) *Inorg. Chem. 40*, 354−360.
76. Adman, E. T. (1991) *Adv. Protein Chem. 42*, 144−197.
77. Adman, E. T. (1991) *Curr. Opin. Struct. Biol. 1*, 895−904.
78. van de Kamp, M., Floris, R., Hali, F. C., and Canters, G. W. (1990) *J. Am. Chem. Soc. 112*, 907−908.
79. van de Kamp, M., Silvestrini, M. C., Brunori, M., Van Beeumen, J., Hali, F. C., and Canters, G. W. (1990) *Eur. J. Biochem. 194*, 109−118.
80. Chen, L., Durley, R., Poliks, B. J., Hamada, K., Chen, Z., Mathews, F. S., Davidson, V. L., Satow, Y., Huizinga, E., Vellieux, F. M. D., and Hol, W. G. J. (1992) *Biochemistry 31*, 4959−4964.
81. Ubbink, M., Ejdeback, M., Karlsson, B. G., and Bendall, D. S. (1998) *Structure 6*, 323−335.
82. Mikkelson, K. V., Skov, L. K., Nar, H., and Farver, O. (1993) *Proc. Natl. Acad. Sci. U.S.A. 90*, 5443−5445.
83. Brooks, H. B., and Davidson, V. L. (1994) *Biochemistry 33*, 5696−5701.
84. Canters, G. W., Kolczak, U., Armstrong, F., Jeuken, L. J. C., Camba, R., and Sola, M. (2000) *Faraday Discuss. 116*, 205−220.
85. Gray, H. B., Malmström, B. G., and Williams, R. J. P. (2000) *J. Biol. Inorg. Chem. 5*, 551−559.
86. Sigfridsson, E., Olsson, M. H. M., and Ryde, U. (2001) *J. Phys. Chem. B 105*, 5546−5552.

BI0117448